Paper published as

Tancredi, U.; Renga, A. & Grassi, M. (2014), 'Geometric total electron content models for topside ionospheric sounding', *Environmental Energy and Structural Monitoring Systems (EESMS), 2014 IEEE Workshop on* 'Environmental Energy and Structural Monitoring Systems (EESMS), 2014 IEEE Workshop on', 1-6.

DOI: 10.1109/EESMS.2014.6923285

Geometric Total Electron Content Models for Topside Ionospheric Sounding

Urbano Tancredi
Dept. of Engineering
University of Naples 'Parthenope'
Naples, Italy
urbano.tancredi@uniparthenope.it

Alfredo Renga and Michele Grassi
Dept. of Industrial Engineering
University of Naples "Federico II"
Naples, Itay
alfredo.renga@unina.it, michele.grassi@unina.it

***Abstract*— The ionosphere is commonly divided into the portion below (bottomside) and above (topside) the region at which peak values of electron density occur. Topside ionospheric modeling is a challenging problem because of the limited data available. Indeed, the more intense peak ionization region, or bottomside ionosphere, dominates the effects observable from ground stations. High-altitude ionosondes, such as sounding rockets, have been traditionally used for direct sounding only of the higher ionospheric layers. Nowadays, signals of opportunity exist for sounding the ionosphere with no dedicated ionosondes. With the continuous deployment of GPS receivers on board spacecraft for positioning, indirect sounding of the topside ionosphere using navigation signals can be performed. This paper reviews geometric-based models allowing to infer the total electron content of the topside ionosphere from spacecraft GPS measurements.**

Keywords—Ionosphere; Space Weather; GNSS; Total Electron Content; Low Earth Orbit; Spacecraft;

I. INTRODUCTION

The portion of the ionosphere above the height at which peak values of electron densities might occur is commonly referred to as the topside ionosphere. Topside ionospheric modeling is a challenging problem because of the limited data available. Indeed, the more intense peak ionization region, or bottomside ionosphere, dominates the effects observable by ground stations. High-altitude ionosondes, such as sounding rockets, have been traditionally used for direct sounding only of the higher ionospheric layers. Nowadays, signals of opportunity exist for sounding the ionosphere with no dedicated ionosondes. With the continuous deployment of GPS receivers on board spacecraft for positioning, indirect sounding of the topside ionosphere using navigation signals can be performed.

The ionosphere affects the propagation of radio electromagnetic waves, introducing a group delay with respect to vacuum conditions. This time delay is related to the total number of electrons encountered by the radio wave on its path, at least to first order [1]. Measuring the time delay induced by the ionosphere on radio signals allows observing this Total Electron Content (TEC) along the ray-path. GPS and, more in general, Global Navigation Satellite Systems – GNSS – allow measuring this time delay (see, e.g. [2], [3]) and, thus to estimate the related TEC. The TEC depends on many factors, including the GPS receiver – Satellite Vehicle (SV) relative geometry, the solar and magnetic activity, local hour, day of year, etc.

One frequent simplification of ionospheric models is to distinguish the effects due to the anisotropy of the electron density from the ones caused by the GPS receiver-SV observation geometry. This is generally achieved by distinguishing the electron distribution along the vertical direction from the one in the horizontal plane. An electron density profile is assumed to exist at any horizontal location, extending from ground to the upper plasmasphere. This vertical profile is then parameterized in order to synthesize its properties in a finite number of parameters. The most common approach is to synthesize the vertical electron distribution into a single parameter, the Vertical Total Electron Content (VTEC), and letting it vary in the horizontal plane. It is thus also often referred to as a 2D model. This 2D VTEC model needs to be complemented by a geometric model capable of estimating the slant ionospheric delay affecting GPS observables. The Vertical TEC is mapped onto the slant one by a multiplicative factor that exploits knowledge of the observation geometry taking into account the increase of the path length in the ionosphere with decreasing apparent elevation of the GPS SV with respect to the user. This term is usually known as the mapping function or obliquity factor.

This paper focuses only on the effects of the user location and the observation geometry, that is, where the GPS Satellite Vehicles (SV) are w.r.t. the receiver. Dependency on other factors is not discussed, and the reader is referred to the relevant literature, such as [1], [4]. Two frequently used, basic mapping functions for ground-based users are considered next, and their adaptation to GPS users in Low Earth Orbit (LEO) is discussed.

II. GEOMETRIC MODELS FOR RECEIVERS ON GROUND

For achieving the separation between the vertical and horizontal electron density distribution, the most common approach is to invoke the so-called shell approximation, presented in [4] and described in some detail in [5]. The shell

model is based on assuming that the electron density is not variable in the horizontal direction along the ray-path between the receiver and the SV. Its use is widespread for ionospheric delays compensation on GNSS navigation signals. Examples of models based on the shell approximation include, but are not limited to, Klobuchar's model [1], which is broadcast along with the GPS navigation message, the Global Ionospheric Maps (GIM) models of NASA Jet Propulsion Laboratory (JPL) [4], and of the Center for Orbit Determination in Europe (CODE) [6].

More specifically, the ionospheric delay I affecting the propagation of a radio signal of frequency f can be approximated to first order to [1]:

$$I = \frac{40.3\ m^3/s^2}{f^2} \cdot TEC$$

where the ionospheric delay is in meters, provided that TEC is expressed in units of electrons/m^2 and the frequency is expressed in Hertz. The TEC is modeled as a function of the electron density along the ray-path, which is assumed straight [5]

$$TEC = \int_{\mathbf{x_r}}^{\mathbf{x^j}} \rho(\theta,\phi,h)\, ds \qquad (1)$$

where the electron linear density, i.e. the numbers of electrons per meter, is denoted as ρ; θ, φ, h stand for Longitude, Latitude and Altitude above Earth's surface; ds stands for the differential of the ray-path length s; $\mathbf{x_r}$, $\mathbf{x^j}$ stand for the receiver and SV j positions.

The shell assumption neglects the horizontal variation of the density along the ray-path, which becomes a function only of the altitude. This function, denoted by $\rho_m(h)$, can be interpreted as the electron density existing at a certain horizontal location, θ_m φ_m, provided that its latitude and longitude are within the ranges spanned by the ray-path (underbar and overbar are used to denote minimum and maximum values, respectively):

$$\rho_m(h) := \rho(\theta_m,\phi_m,h) \approx \rho(\theta,\phi,h)$$
$$\forall\{\theta,\phi\} \in \left[\underline{\theta},\overline{\theta}\right]\times\left[\underline{\phi},\overline{\phi}\right], \{\theta_m,\phi_m\} \in \left[\underline{\theta},\overline{\theta}\right]\times\left[\underline{\phi},\overline{\phi}\right] \qquad (2)$$

The integrand in Eq.(1) thus becomes a function only of the altitude, as well. It is convenient to change the integration variable from the path length to the altitude. Applying Carnot's theorem to the triangle R+h, R, s shown in Fig. 1 we obtain:

$$s = -R\sin E + R\sqrt{(1+h/R)^2 - \cos^2 E} \qquad (3a)$$

$$ds = \frac{dh}{\cos\gamma} \qquad (3b)$$

$$\cos\gamma = \frac{R}{R+h}\sqrt{(1+h/R)^2 - \cos^2 E} \qquad (3c)$$

$$M_{TS}(E,h) = 1/\cos\gamma \qquad (3d)$$

where the M_{TS} function is the thin shell mapping function, for reasons that will be explained later on, γ stands for the local zenith angle at altitude h, and R for Earth's radius (see Fig. 1).

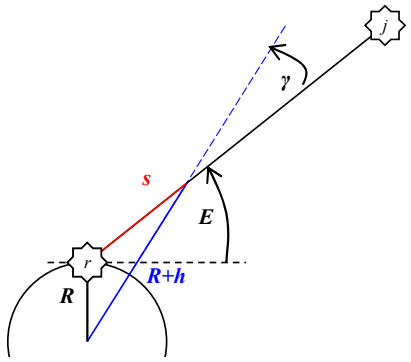

Fig. 1. Relationship between ray-path length s and altitude h

The TEC expression (1) for the shell model specializes thus to

$$TEC = \int_{h_r}^{h^j} \rho_m(h)\, M_{TS}(E,h)\, dh \qquad (4)$$

Consider now the total electron content for a vertical ray-path, i.e. the Vertical TEC (VTEC). Without introducing any assumption, if we denote as θ_m φ_m the horizontal location of the receiver, we can write from Eq.(1) that:

$$VTEC(\theta_m,\phi_m) = \int_{h_r}^{h^j} \rho_m(h)\, dh \qquad (5)$$

Combining this exact formula (5) with the shell model one (4) one obtains:

$$TEC = M(E)\cdot VTEC(\theta_m,\phi_m) \qquad (6a)$$

$$M(E) = \frac{\int_{h_r}^{h^j} \rho_m(h)\, M_{TS}(E,h)\, dh}{\int_{h_r}^{h^j} \rho_m(h)\, dh} \qquad (6b)$$

where we have introduced the mapping function $M(E)$. Eq.(6) define the shell model approximation. The shell model allows separating the effects of the horizontal position of a point (belonging to the ray-path) from the ones due to the elevation of the satellite above the receiver's horizon. The altitude of the receiver is mathematically constrained only to be smaller than the SV altitude. This model, however, still requires integration of the linear electron density along the ionosphere shell's altitude for computing the mapping function. Additional assumptions shall be introduced to obtain an algebraic form of Eq.(6) by solving the two integrals. The next two sections discuss two possible alternatives.

A. Thin Shell Model

For obtaining a closed-form algebraic expression of the mapping function in lieu of Eq.(6), one approach is to introduce the ***thin*** shell assumption, so called because it concentrates the whole ionosphere in a shell of infinitesimal thickness at a certain altitude. The thin shell model is a simple

variation of the general shell model. It is also frequently referred to as the Single Layer ionospheric Model (SLM), and is also the reference approach used for 2D modeling of the ionosphere (a thorough review of its application is available in [7])

More precisely, in addition to the shell model's assumptions, the thin shell model supposes the electron density to be almost everywhere null, except at an altitude h_{TS}. The altitude profile of the electron density can be then expressed in terms of the Dirac delta function, and, as a consequence, the mapping function becomes equal to $M_{TS}(E)$:

$$\rho_m(h)\big|_{TS} = \rho \cdot \delta(h - h_{TS}) \qquad (7a)$$

$$TEC \approx M_{TS}(E, h_{TS}) VTEC(\theta_m, \phi_m) \qquad (7b)$$

A substantial difference with the general shell model is that both the latitude and the longitude ranges of Eq.(2), within which one must select θ_m φ_m, degenerate in a singleton. This single point is given by the intersection of the ray-path with the thin shell, which is called Ionospheric Piercing Point (IPP). Its coordinates depend on the receiver position, on the SV elevation, and on the azimuth angle. Examples of techniques for computing the IPP coordinates are available in [1] and [4]. We emphasize that the VTEC in Eq.(7b) will not be the total electron content of the column above the receiver, but will refer to a different horizontal position, given by the IPP. If the model is used for estimating an horizontally-varying VTEC map, such as in [5], it should be taken into account that measurements from the same receiver will sample the VTEC over different geographical locations. On the other hand, if a single VTEC is used for predicting slant TEC from different SV to the same receiver, one is implicitly assuming the VTEC to be equal in all the piercing points relevant to the different SV.

B. *Thick Shell Model*

Several alternatives to the thin shell model exist. A similar approach is to model the ionosphere as confined within a shell of finite thickness, yielding a thick shell or slab model. This approach has been used by NASA JPL in the past decades [8] and has found additional applications [9],[10]. The thick shell model consists in adopting the shell approximation of Eq.(6) and making the following additional assumptions:

i. the ionosphere is confined into a spherical shell of thickness $\Delta h = h_M - h_m$,
ii. the electron density is uniformly equal to ρ inside the shell and null outside
iii. the receiver is at null altitude and the signal fully crosses the ionosphere, i.e. $h_r = 0 \le h_m$ and $h_M \le h^j$ (see Fig. 2.)

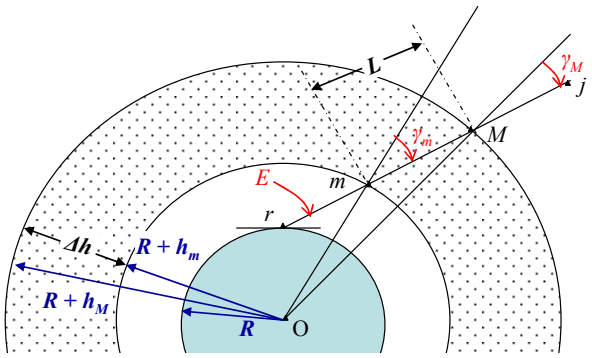

Fig. 2. Thick shell model geometry – Ground based receiver

As such, the shell model's mapping function of Eq.(6) specializes to

$$M(E) = \frac{1}{\Delta h}\int_{h_m}^{h_M} M_{TS}(E,h)\,dh = \frac{1}{\Delta h}\int_{s_m}^{s_M} ds$$
$$= \frac{R}{\Delta h}\left[\sqrt{(1+h/R)^2 - \cos^2 E}\right]_{h_m}^{h_M} \qquad (8)$$

Thus, the mapping function for a thick uniform shell depends only on the shell minimum and maximum altitude, other than on the elevation of the SV w.r.t. the receiver. By Eq.(3b), the mapping function for the uniform thick shell can also be interpreted as the ratio between the ray-path length $L = s_M - s_m$ and the shell's slant thickness (Fig. 2).

A comparison can be performed with the thick shell model proposed in [10], where the following expression is given, even though with no proof.

$$M(E) = \frac{2(1+\Delta H/2)}{\sin\varepsilon_m + \sqrt{\sin^2\varepsilon_m + 2\Delta H + \Delta H^2}} \qquad (9)$$

where $H = h/R$, $\Delta H = \Delta h/R$, and ε_m is the elevation w.r.t. local horizon at the point the ray-path intersects the shell's lower border, which is complementary to the local vertical γ_m , i.e. $\varepsilon_m = \pi/2 - \gamma_m$ (Fig. 2). Applying the law of sines to the *Orm* triangle in Fig. 2, the elevation at the shell border can be related to the ground-based receiver elevation by:

$$\cos\varepsilon_{m(M)} = \frac{\cos E}{1 + H_{m(M)}} \qquad (10)$$

The mapping function given in Eq.(9) is not perfectly equal to the one of Eq.(8), even though the differences are in the order of 1 percentage point at most. This is because Eq.(9) performs additional simplifications based on the h/R term magnitude for ground-based receivers, as discussed in next section. Because of the simplicity of Eq.(8), and to extend the model to space-based receivers, these simplifications are not necessary herein.

III. Adapting Models to Receivers in Space

The models described in the previous section explicitly assume the receiver to be on ground, and shall thus be adapted

to a receiver at non-zero LEO altitude. The next sections discuss such modifications.

Several mapping functions have been developed for spaceborne GPS receivers. The empirically-derived mapping function proposed by Lear in [11] has reportedly shown good prediction capabilities (see, e.g. [2],[11]–[14]) and is thus taken as a reference.

A. Thin and Thick Shell Models

The thin shell mapping function of Eq.(7) does not strictly require the receiver to be on ground, i.e. at a distance R from Earth's center. The only necessary condition for obtaining Eq.(7) is that the receiver shall be below the ionosphere thin shell height, that is, it implicitly assumes that:

iv. The receiver is at an altitude lower than or equal to the thin shell altitude, $h_r \le h_{TS}$.

Indeed, if assumption **iv** does not hold true, Eq.(6b) becomes undetermined, and the thin shell model Eq.(7) is not valid any more. Provided that assumption iv holds true, the thin shell mapping function M_{TS} has to be modified for taking into account the receiver's altitude. Indeed, the local zenith angle dependency on E, Eq.(3c), is valid if and only if the elevation angle E is taken with respect to a point on the Earth's surface. This is because the altitude h is defined w.r.t. the point at which the elevation is taken. In light of this remark, M_{TS} can be obtained by keeping Eq.(3d), but modifying the zenith angle dependency using the elevation at the (non-zero) receiver's altitude. Expressing the thin shell altitude as the delta w.r.t. the receiver's altitude, $h'_{TS} = h_{TS} - h_m$, and increasing the 0-altitude sphere length R accordingly, $R' = R + h_m$, the zenith angle dependency on elevation modifies into:

$$\cos\gamma = \frac{R'}{R'+h'}\sqrt{\left(1+h'/R'\right)^2 - \cos^2 E} \qquad (11a)$$

Concerning the thick shell model, assumption i and ii are independent of the receiver's altitude, whilst assumption iii is dropped and substituted by the following

v. The receiver is at an altitude equal to the shell lower border, i.e. $h_r = h_m$ and $h_m \le h_j$.
vi. The SV is above the receiver's local horizon, i.e. $E \ge 0$ deg.

The above assumptions allow including typical LEO applications. Indeed, typical altitudes of the shell lower border altitude are in the order of 100 km, 200 at most, which is significantly below the lowest usable LEO altitudes. Negative elevation SV are generally discarded, because of the low measurement quality. As such, the portion of the shell that is below the receiver is unessential, and one can consider the simpler case of assumptions **v**,**vi** (see Fig. 3)

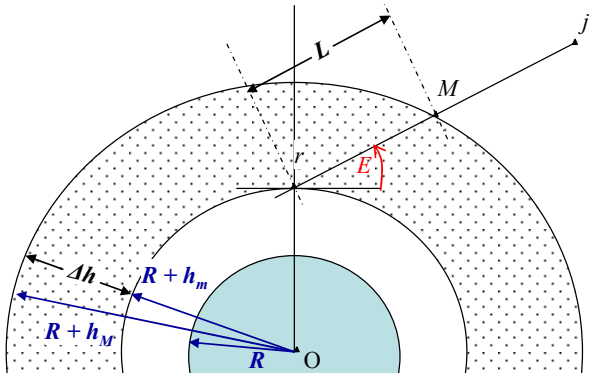

Fig. 3. Thick shell model geometry – Space based receiver

Proceeding as for Eq.(8) and introducing the ratio of the altitude w.r.t. Earth's surface h to the receiver's altitude sphere radius as $\eta = h/R'$, yields the following mapping function

$$M(E) = \frac{2(1+\Delta\eta/2)}{\sin E + \sqrt{\sin^2 E + 2\Delta\eta + \Delta\eta^2}} \qquad (12)$$

Eq. (9), (12) are formally analogous (the elevation angle ε_m is identical to E in this case). This analogy allows a simple interpretation of Spilker's formula Eq.(9), which neglects the shell's lower border altitude w.r.t. Earth radius. Note also that as the shell thickness goes to zero, Eq.(12) reduces to Eq.(11) with $h_{TS} = h_m$, as expected. Even though this remark might suggest that the thick shell model is a generalization of the thin one, this can be misleading. Indeed, because of the uniform electron density assumption, all signals coming from different SV at the same elevation angle induce the same slant TEC in the thick shell model. The thin shell model, instead, is capable of taking into account the different relative azimuth of the SV with respect to the receiver, via the IPP position. This is an advantage especially when dealing with low-elevation satellites, for which the regions of ionosphere crossed by ray-paths of SV at similar elevations can be quite far from each other depending on the relative azimuth. In this sense, the thin shell model has a broader capability of ionospheric delay modeling than the thick shell one.

B. Comparison with Reference Model

As previously discussed, the empirical mapping function proposed by Lear in [11] represents a term of reference for predicting ionospheric delays [2] in LEO. The empirical mapping function proposed by Lear is:

$$M(E) = \frac{2.037}{\sin E + \sqrt{\sin^2 E + 0.076}} \qquad (13)$$

The model has been empirically derived and it is suitable to vertical delays mapping for elevation angles above 5 deg. at LEO altitudes [11]. Eq.(13) has the same analytical structure of the thick shell model of Eq.(12). Comparing the two mapping functions, they coincide if the following matching conditions hold, which are exemplified for a few realistic scenarios in Table 1:

$$\begin{cases} 2(1+\Delta\eta/2) = 2.037 \\ 2\Delta\eta + \Delta\eta^2 = 0.076 \end{cases} \quad (14)$$

TABLE I. SAMPLE SHELL ALTITUDES AND THICKNESS FOR ENSURING MATCHING CONDITIONS

h_m , km	h_M , km	Δh , km
350	598.9	248.9
450	702.6	252.6
550	806.3	256.3

Hence, Lear's mapping function yields the same results of the thick shell model for receivers in space, Eq.(12), provided that the matching conditions (14) are satisfied. As such, Lear's mapping function can be reasonably assumed to arise from a thick shell model, particularized for a certain (h_m,h_M), which obey the matching conditions. Fig. 4 shows the effects of varying the shell parameters on the thick shell mapping function. The shell lower altitude has a very limited influence on the mapping function, whereas a substantial difference at low elevations exists for varying shell thickness.

At last, a comparison is made between the thin and thick shell mapping functions, i.e. Eq.(11) vs. Eq.(12). Note that, in order for the two models to be comparable, the same receiver's altitude shall be selected, and the thin shell altitude is expected to be within [h_m, h_M] for theoretical consistency. As shown in Fig. 5, the thin shell mapping function can be made quite similar to the thick shell one. In particular, for a receiver altitude of 450 km, Lear's mapping function, corresponding to a thick shell model with a thickness of about 250 km (bold curve in Fig. 5), can be approximated by a thin shell model with h_{TS} = 550 km. This approximation is accurate, even though discrepancies in the order of O(10 %) can occur for elevation angles below 10 deg.

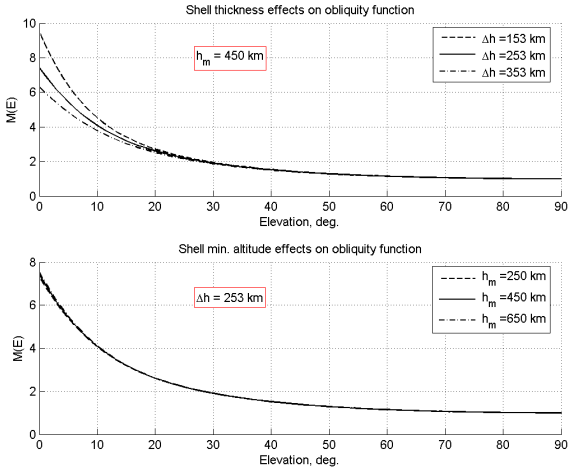

Fig. 4. Mapping function dependency on shell parameters.

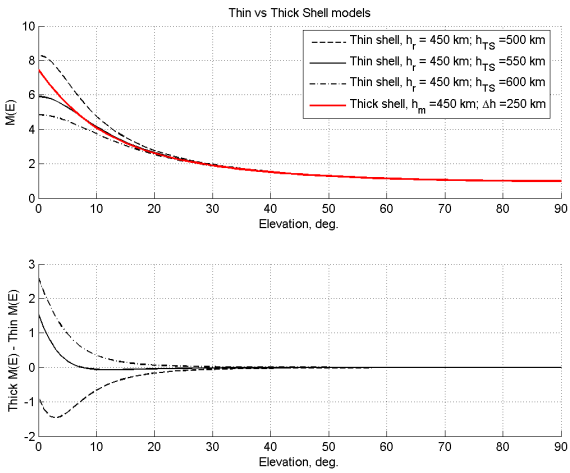

Fig. 5. Thin vs. Thick shell mapping functions for spaceborne receivers.

IV. CONCLUSION

This paper has revisited the main steps, the analytical expression, and the underlying assumptions of most common geometry-based ionospheric models. Geometry based models come into play thanks to simplifying assumptions on the distribution of the electron density along the ray-path. In the simplest case of uniform electron density within a spherical shell (both vertically and horizontally), the geometry becomes the only effect to take into account for computing the slant to vertical TEC ratio, also known as the mapping function or obliquity factor. In the thin shell model, the shell has infinitesimal thickness, and this allows to broaden the model for including dependency of the electron density on the horizontal position. In this way, the global VTEC maps distributed by the International GNSS Service – IGS can be built.

The models have then been extended to the case of a space –based GNSS receiver. Lear's mapping function, a term of reference for space applications, matches the one of a thick shell model, referring to a shell of specific geometric properties. Evaluating the matching conditions, which allow aligning Lear's mapping function to the general thick shell one, suggests that Lear's model refers to a shell of ~250 km thickness for receiver altitudes between 350 and 550 km.

The thick shell mapping function heavily depends on the shell thickness for elevations lower than 20 deg., and loosely on the minimum altitude of the shell. Taking into account that receivers in LEO will be above the shell's minimum altitude, the receiver's altitude will determine the effective shell thickness. As such, the receiver's altitude shall be correctly taken into account in formulating the mapping function, especially if low elevation SV are used.

The thin shell model can provide a mapping function which is very close to Lear's one as well, depending on the thin shell altitude chosen, at least for SV sufficiently high above the horizon (not less than 10 deg. of elevation).

At last, it is emphasized that the notion that the VTEC estimated by ionospheric delay measurements from a space based receiver represents the electron content of the vertical column above the receiver is erroneous. In a thick shell model, the estimated VTEC rather represents a mean among the VTEC in the surroundings of the receiver, weighted by the thick shell mapping function. In a thin shell approximation, the VTEC represents instead the electron content of the vertical column at the position of the Ionospheric Piercing Point, where the signal's ray-path intersects the thin shell.

REFERENCES

[1] Klobuchar, John A. "Ionospheric time-delay algorithm for single-frequency GPS users." Aerospace and Electronic Systems, IEEE Transactions on 3 (1987): 325-331.

[2] Tancredi, U., Renga, A., & Grassi, M. (2011). Ionospheric path delay models for spaceborne GPS receivers flying in formation with large baselines. Advances in Space Research, 48(3), 507-520.

[3] Bondavalli, A., Ceccarelli, A., Gogaj, F., Seminatore, A., & Vadursi, M. (2013). Experimental assessment of low-cost GPS-based localization in railway worksite-like scenarios. Measurement, 46(1), 456-466.

[4] Mannucci, A.J., B.D. Wilson, and C.D. Edwards (1993) "A new method for monitoring the earth ionospheric total electron content using the GPS global network" Proceedings of ION GPS-93, pp.1323-1332

[5] Mannucci, A. J., B. A. Iijima, U. J. Lindqwister, X. Pi, L. Sparks, and B. D. Wilson (1999), GPS and ionosphere, in Reviews of Radio Sci., 1996–1999, edited by W. R. Stone, Oxford Univ. Press, New York.

[6] Schaer, S., G. Beutler, M. Rothacher, and T.A. Springer, Daily Global Ionosphere Maps Based on GPS Carrier Phase Data Routinely Produced by the CODE Analysis Center, Proceedings of the IGS AC Workshop, Silver Spring, MD, USA, March 19–21, 1996, pp. 181–192.

[7] Mitch, R. H., M. L. Psiaki, and D. M. Tong (2013), Local ionosphere model estimation from dual-frequency global navigation satellite system observables, Radio Sci., 48, 671–684, doi:10.1002/2013RS005153.

[8] Coster, A., Gaposchkin, E., Thornton, L. Real-Time Ionospheric Monitoring System Using the GPS, Proceedings of the 4th International Technical Meeting of the Satellite Division of The Institute of Navigation (ION GPS 1991), Albuquerque, NM, September 1990, pp. 299-308.

[9] Xu, G. GPS. Theory, Algorithms and Applications. Springer, 2nd ed. 2007.

[10] Spilker, J.J. (1996), GPS Navigation Data, Global Positioning System: Theory and applications. Vol. 1 (A96-20837 04-17), Washington, DC, American Institute of Aeronautics and Astronautics, Inc. (Progress in Astronautics and Aeronautics. Vol. 163), , p.121-175

[11] Lear W.M. (1988), GPS navigation for low Earth orbiting satellites, NASA Lyndon B. Johnson Space Center, Mission planning and analysis division, 1st revision, 87-FM-2.JSC-32031.

[12] van Barneveld, P., Montenbruck, O., Visser, P. Epochwise prediction of GPS single differenced ionospheric delays of formation flying spacecraft. Advances in Space Research, 44, 987–1001, 2009.

[13] M. Garcia-Fernàndez and O. Montenbruck, "Low earth orbit satellite navigation errors and vertical total electron content in single-frequency GPS tracking," Radio Science, Vol. 41, RS5001, 2006

[14] Tancredi, U., Renga, A., & Grassi, M. (2013). Real-Time Relative Positioning of Spacecraft over Long Baselines. Journal of Guidance, Control, and Dynamics, 37(1), 47-58.